http://dx.doi.org/10.15576/GLL/2022.3.103

GLL

Geomatics, Landmanagement and Landscape No. 3 • 2022, 103–115

KARSTIC LANDSCAPE DETECTION USING ELECTRICAL RESISTIVITY TOMOGRAPHY IN NORTHEAST ALGERIAN

Serhane Brahmi, Fehdi Chemseddine, Riheb Hadji, Smail Brahmi, Amor Hamad, Younes Hamed

Summary

Sinkhole (doline) collapse is one of the major natural hazards threatening people and property in the Middle East and North Africa (MENA) region, especially if the bedrock structure is epi-karstic, covered by encrusted material. Many dolines-avens collapses have been recorded in urban and rural areas in Northeast Algeria. Our study identifies localized deformation that may be caused by a sinkhole activity based on the electrical resistivity tomography (ERT) imaging in Setifian high plains. For this task, we conducted 2-D Wenner and Wenner-Schlumberger transects profiles. The geological and hydrogeological study helped to calibrate the resistivity model, and in this regard, expound on the proneness of the limestone layer to collapse. The obtained model highlights the heterogeneity of the subsurface. The inverted transects allowed the investigation of 20 m depth with Wenner array and 52 m with Wenner-Schlumberger. The Wenner inverted models imaged the chimney and different karst networks until 20 m depth; even as the Wenner-Schlumberger models imaged a new karstic cavity in the limestone layer. ERT imaging has once again proven its effectiveness in mapping sinkholes based on its ability to detect resistivity. Our research can certainly benefit karst collapse monitoring in other areas of the high plain region.

Keywords

natural hazards • doline • geophysical survey • resistivity • underground voids

1. Introduction

Countries in the MENA region are becoming increasingly vulnerable to geological hazards, namely, floods, earthquakes, slope movements, and Sinkhole collapse [Hadji et al. 2013; El Mekki et al. 2017; Anis et al. 2019; Brahmi et al. 2021; Hamad et al. 2021]. Their mitigation requires the recognition of the high susceptible areas, based on the distribution of predisposing and triggering factors [Ford and Williams 2013; Hadji et al. 2014a, b, 2016, 2017; Chemseddine et al. 2015; Hamed et al. 2017a, b, 2022; Dahoua et al. 2017 a, b; Manchar et al. 2018; Fredj et al. 2020; Besser et al. 2021; Hamad et al. 2021]. The underground water runoff process along channels in the fracture's dissolves closed depressions in the bedrock. These sinkholes are a characteristic feature of karstic landscapes in a carbonate environment. Cave roof collapse can spread out to the surface forming thus a collapse sinkhole (Fig. 1) [Fehdi et al. 2011; Ford and Williams 2013; Zahri et al. 2016; Hamad et al. 2018a, b; Mahdadi et al. 2018; Hamed et al. 2018]. This is the case with the terrain of the Setifian high plains, where these ground movements keep causing damage.

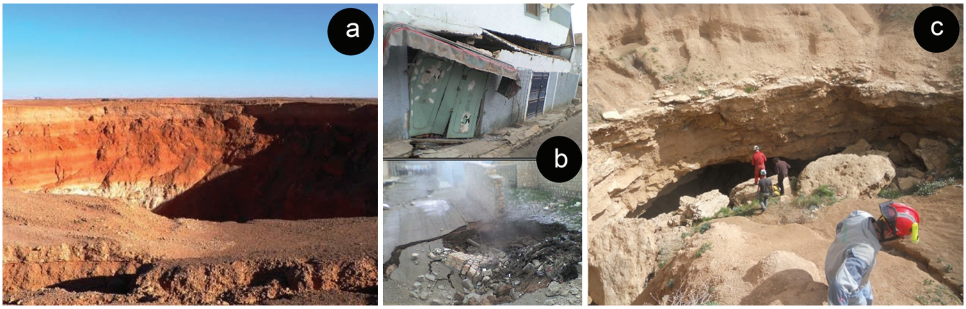

Source: Mouici et al. [2017]

Fig. 1. a) The collapse of Haoud Berkaoui with a crater of 350 m depth (Sahara, Algeria), b) The collapse in Cherea City (NE Algeria); c) The collapse in Drâa Douamis (NE Algeria)

A sinkhole is widely known as a morphological depression in the ground that has no natural external surface drainage. The development of grooves and cavities results from the physicochemical dissolution process of the rainwater charged with atmospheric carbon dioxide on limestones, dolostones, gypsum, halite, and sylvite; leading to the dissolution of the calcium carbonate into bicarbonate [Khaldaoui et al. 2015; Mokadem et al. 2016; Besser et al. 2018; Zeqiri et al. 2019; Ncibi et al. 2020 a, b, 2021].

Extant literature has provided an insightful understanding of the distribution and genesis of karst collapses [Mouici et al. 2017]. *In situ* geophysical techniques such as electrical resistivity tomography (ERT), ground-penetrating radar (GPR), electromagnetic (EM), seismic refraction (SR), and micro-gravimetry (MG)... are the most widely used for monitoring and early warning of cover-collapse sinkholes in Karst-terranes landscapes [Nouioua et al. 2013; Watlet et al. 2018; Brahmi et al. 2021]. Whereas direct techniques such as drilling, coring, and standard penetration test... are used in predicting underground Karstic voids and roof collapses for land use plans [Raïs et al. 2017; Saddek et al. 2019].

Tomography imaging based on electrical resistivity is a suitable method for underground void detection. Since they are usually filled with water or inconsistent material, with differential resistivity than the host rocks, the ERT is markedly adapted to investigate these grooves and cavities [Kidanu et al. 2016; Giampaolo et al. 2016].

A successful case study demonstrating cavity detection using ERT conducted in dolomitic rocks near Pretoria, South Africa was reported by Van Schoor [2002]. Talib et al. [2022] have studied the detection of sinkhole activity in West-Central Florida using radar interferometry and GPR and ERT surveys. Gaballah and Alharbi [2022] applied 3-D GPR visualization integrated with the ERT technique for characterizing near-surface fractures and cavities in limestone. The Wenner configuration is suited for stratified terrains, allowing a high-quality vertical resolution, but with a limited investigation-depth. The dipole-dipole configuration is more suitable for vertical structures [Dahlin and Zhou 2004]. Nevertheless, the Wenner-Schlumberger configuration could be used for both structures.

This work highlights the usage of an imaging technique that was demonstrated to be effective in the identification of sinkhole structures. It allowed the investigation of the Advantages and limits of sinkhole monitoring from scientific, practical, and technical points of view. The results obtained in our research will help to solve many engineering geologic problems in complex situations, especially in urbanized areas.

2. General setting

The study area is in the Setifian high plains region between 5°75' to 6°25' N longitude and 36°00' to 36°33' E latitude. It is situated at two kilometers South of El Welja chief-town, Setif province, NE Algeria (Fig. 2). The stream flow is divided among the Chott Beïda endorheic and the Rhumel exoreic basins. Who intermittent and ephemeral streams mark the area [Karim et al. 2019]. The climate of the basin is semi-arid, with 400 mm/year of average precipitation, 16.5°C of average temperature and an acute evapotranspiration potential [Demdoum et al. 2015]. The study site belongs to fractured carbonatic outcrops of the Pleistocene age. The water table levels fluctuated from 28 m in depth in spring to 25 m in autumn. The shallow aquifer suffers from acute overexploitation in the valley and irregularity of precipitation [Benmarce et al. 2021]. The severe lowering of the water table is the main triggering factor for the collapse of this epikarstic terrain.

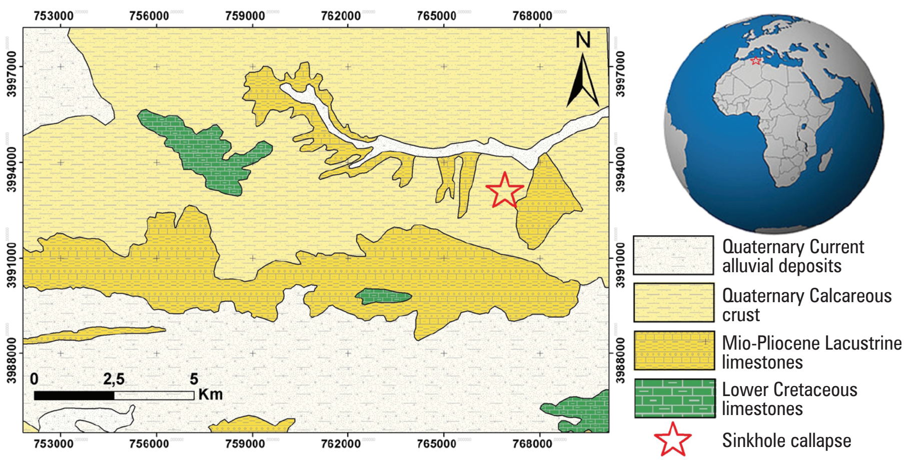

Source: Authors' own study

Fig. 2. Simplified geologic map of the study area

The study area consists of Neogene sediments with clayey, silty, and sandy material (Fig. 3a, b, 4e, and 4f). These facies cover up a fractured limestone formation, which favored the karstification process. The main collapse occurred in 2017 with an elliptical crater of 35 by 26 m, 17 m depth, and N-S orientation. It resulted from suffusion of the roof material, consequential to a dissolution process.

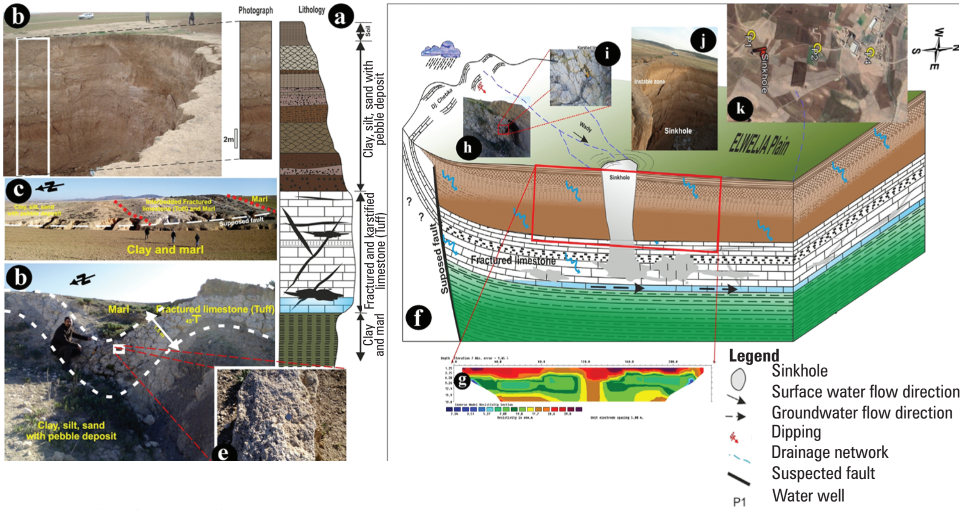

Source: Authors' own study

Fig. 3. Left: a) Simplified facies stratification; b) Lithology of the collapse; c) Inter-bedded karstified limestone and marl of Jebel Chebka; d and e) Fractured limestone with indication of the dipping degree; f) Conceptual model of the study area; g) Pseudo section of the sinkhole chimney; h) and i) Fractured and karstified limestone; j) Photo showing the inside of the collapse; k) Position of the water wells

3. Materials and methods

Extensive fieldwork permitted the data acquisition and the terrain characterization of the geometry, the geological nature, and hydrogeological conditions of the collapse (Figs. 3f-k). This allowed determining the most suitable geophysical acquisition device, able to reach targets deeper than 20 m. We used a SYSCAL Pro Standard & Switch (48) Version 10 channel resistivity-meter for resistivity device (Fig. 4c). The operating mode of the ERT technique is based on the varying electrical resistivity (in Ωm) of the subsurface materials. The conductivity values depend on bedrock type, permeability, cation exchange, alteration, water to host-rock interaction, fracturing, etc. We have chosen survey lines based on the groundwater flow-direction (Fig. 4 a). In the Wenner and Wenner-Schlumberger arrays, we used RES2-Dinv software to delineate shapes and enhance the signal-to-noise ratio (Table 1).

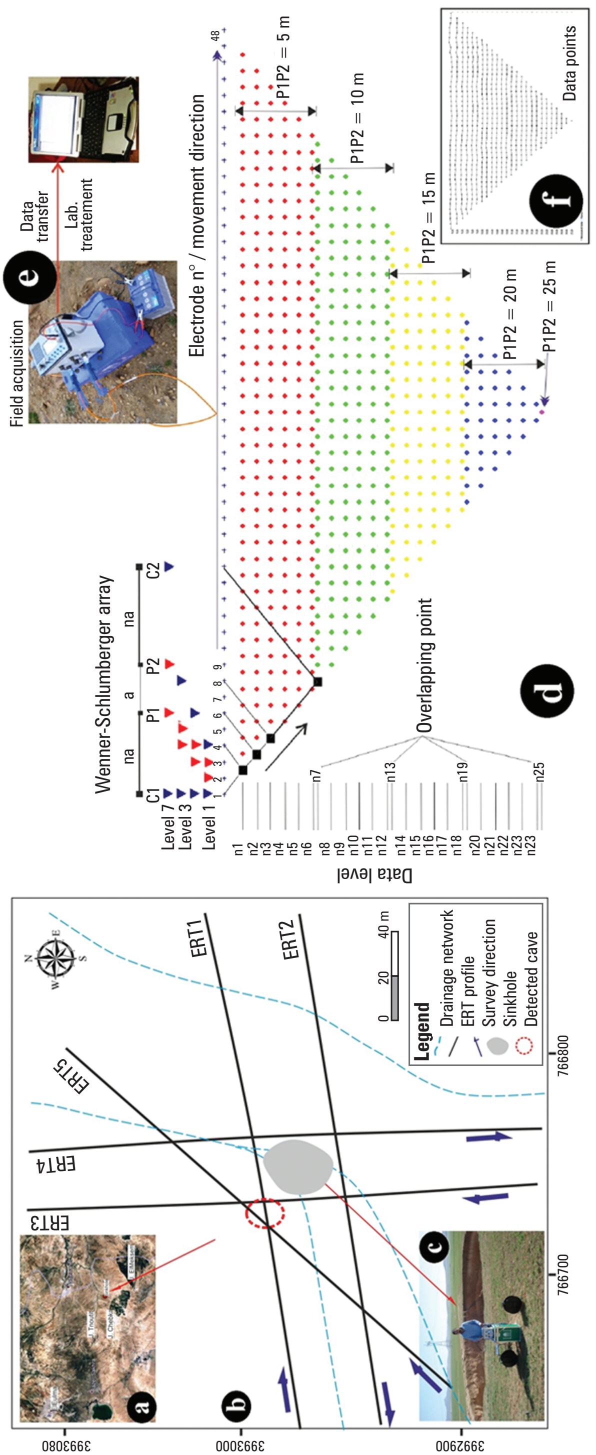

Source: Authors' own study

Fig. 4. a) Location of the study area in El Weldja plain; b) Position of the ERT lines all around the sinkhole; c) Photo showing acquisition of ERT1; d) Schematic diagram of the Wenner-Schlumberger array electrode configuration; e) Field acquisition and lab. Data treatment: f) Data points of the ERT5 displayed using the "Exterminate bad data points" RES2DINV option

Table 1. ERT Transects Characteristics, Electrode spacing = 5 m, Number of electrodes = 48

ERT array configuration	Wenner				Wenner- Schlumberger			
	ERT1	ERT2	ERT 3	ERT 4	ERT 1	ERT 3	ERT 4	ERT 5
Number of levels	6				25			
Reference resistivity	16.524	16.577	16.793	16.962	15.522	15.633	15.352	15.431
Average sensitivity	1.413	1.432	1.414	1.376	3.103	1.253	1.260	1.246
Resistivity contour	Logarithmic intervals							
Min apparent resistivity [Ωm]	11.58	11.39	11.58	10.37	11.65	10.34	8.97	10.63
RMS error [%]	1.17	1.19	1.45	1.52	1.96	0.95	2.60	0.88

The operating mode consists of the injection of an electric current through C1 and C2 electrodes and the measurement of the current potential with P1, and P2 electrodes. This potential varies according to the geophysical characteristics of the terrain. The resistivity of the ground is obtained by running the standard least-squares algorithm. We arranged a transect profile with 48 electrodes of 5 m spacing (Fig 4d). We used the Electre pro-2016 to make sequences with the required depth investigation. Thus, we applied different combinations of a-spacing, and n-separations to increase the density of the data measurement points and optimize the signal-to-noise ratio. The study site is far away from any source of electrical noise, which gives excellent SNR resistivity [Zhu et al. 2017]. We realized four (04) Wenner and Wenner-Schlumberger array transect around the sinkhole in February 2017 (ERT1 to ERT4) (Fig. 4 a, b). We added a fifth line in May 2017, to visualize the noticed cavity in the previous inversion. We inverted data using the RES-2Dinv software to get 2D imaging of the investigated section (Fig. 5e, f). The obtained pseudosection of true resistivity is reached after seven iterations. The root-mean-square (RMS) value rages between 0.88 and 2.4%.

4. Results and discussion

The five ERT profiles (Fig. 5) showed a noteworthy step up between the measured data and the calculated one. The result of inversion schemes the underground structure architecture around the collapsed hole. We have arranged the Wenner transects at 10 m (E-W and N-S) far from the hole (Figs. 5 a, b, c, d). We calibrated the conceptual model by taking considering the facies of the sinkhole wall. The model reveals an intercalated alluvium layer of four m thick gave resistivity of 36 Ωm. A silt-clay layer of 18 m thick gave resistivity less than 20 Ωm. The Wenner-Schlumberger profile highlighted a tuffaceous limestone formation with resistivity exceeding 65 Ωm. This fractured and karstified layer constitutes the shallow aquifer of 18 m to 28 m depth, overcoming the clayey substratum over 28 m depth (Fig. 5e). According to the ERT 1 inversion (52-m depth, with 0.0196 RMS), a new void of 10 m height, was detected between electrodes 18 and 22 at 28 m depth (Fig. 5e). This karstic cavity is developed in the limestone layer. The S-N and N-S oriented ERT lines (Figs. 5f and 5g), gave an RMS of 0.95% to 2.6% after 5 to 7 inversions. The pseudo-sections revealed a resistivity variation of the limestone layer according to the fracturing degree. The Wenner-Schlumberger intersects showed elevated resistivity contrasts from 18 m to 28 m depth, among the 23rd and 28th electrode (Fig. 5h).

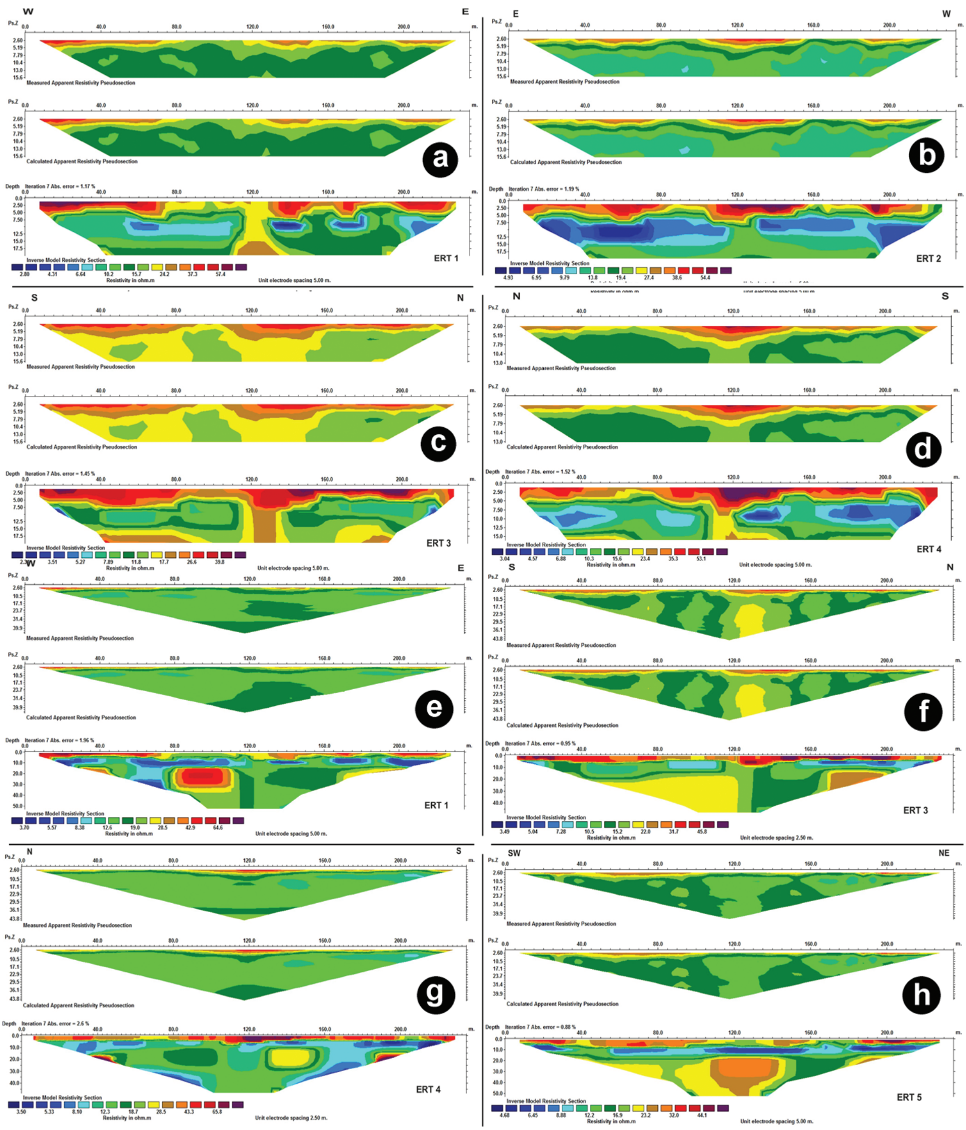

Source: Authors' own study

Fig. 5. Inversion of ERT by Wenner transect: a) ERT 1, b) ERT 2, c) ERT 3, d) ERT 4. Inversion of ERT by Wenner-Schlumberger transect, e) ERT1, f) ERT2, g) ERT3, h) ERT4

This anomaly unveiled a new cavity connected to the existing one. The low resistivity in the tuffaceous limestone, observed in the ERT 1 (Fig. 5e) and ERT 5 (Fig. 5f), proves the filling of karst networks with clayey-silty material. The inversion values increase with a ratio of 1.7 and 1.5, out of the imaging domain [Zhu et al. 2017]. In the inverted model, ERT 1 (Fig. 5f) and ERT 5 (Fig. 5g) high resistivity provided the geometry of the newly discovered cavity.

A chimney sinkhole of 18 m depth was imaged with the Wenner inversion model in the ERT 1 to ERT 4 lines. This shape is not well clear in the Wenner-Schlumberger inverted model. This is due, to the moderate sensitivity of the Wenner-Schlumberger array, and to the ratio of the vertical/horizontal scale for both inverted models. Sensitivity is a measure of how well the resistivity in each part of the model can be resolved by the data collected. Sensitivity values are unitless and are normalized by dividing by the mean and the measured data of the resistivity survey [Loke et al. 2014]. Excluding for the ERT 5 transect; all the inversion models showed the sinkhole chimney (Fig. 6a).

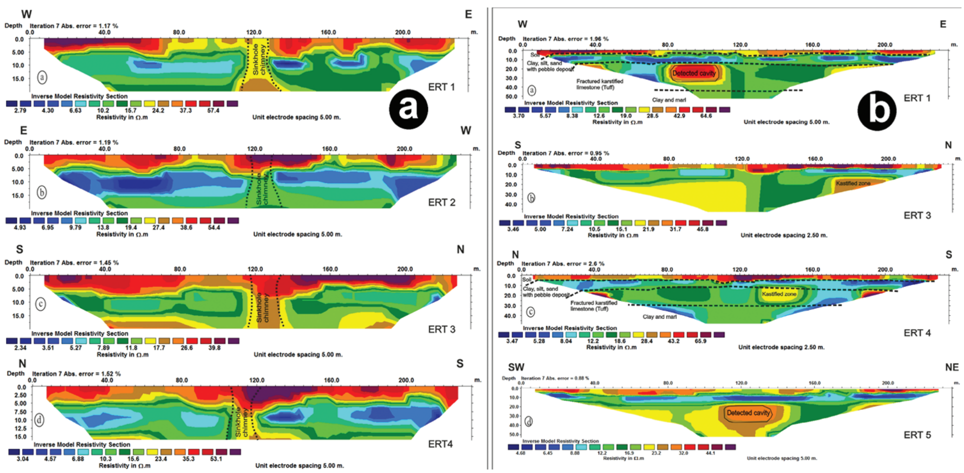

Source: Authors' own study

Fig. 6. a) Inversion of electrical resistivity tomography by Wenner transects showing in dashed line the actual position of the sinkhole chimney, b) Inversion of electrical resistivity tomography by Wenner-Schlumberger transects showing in dashed line the approximate limits of the geological units

In the same context, a new cavity contrast was shown by ERT 1 and ERT 5 inverted models of the Wenner-Schlumberger transect (Fig. 6b).

Our study demonstrated once again that the same causal factors control the genesis and collapse of karst cavities in the semi-arid environments of northeastern Algeria. The works of Nouioua [2013], Mouici et al. [2017] confirm the obtained results. The present study has described the application and advantages/disadvantages of the ERT method, which should be used for all its sinkhole claim investigations. The Wenner configuration is useful for shallow investigations, whereas the Wenner-Schlumberger configuration is useful for the deepest investigations.

5. Conclusion and recommendations

Our study has established the effectiveness of the ERT imaging technique for detecting doline and cavities, in semi-arid climate regions. The underground water flow charged in atmospheric carbon dioxide along the fracture network of the carbonate bedrock causes the dissolution of the calcium carbonate into bicarbonate and thus the formation of sinkholes. Datasets acquisition is achieved with high SNR conditions (a low electrical noise, a minimum contact resistance, and a maximum transmit current). The Wenner profiles are more useful for shallow investigations, whereas the Wenner-Schlumberger configuration for the deepest investigations. The obtained model highlights the heterogeneity of the terrain. The inverted transects allowed the investigation of 20 m depth with Wenner array and 52 m with Wenner-Schlumberger. The Wenner inverted models imaged the chimney and different karst networks until 20 m depth; whilst the Wenner-Schlumberger models imaged a new karstic cavity in the limestone layer. Geologic and hydrogeological investigations helped calibrate the resistivity model. Such sinkhole development can be mitigated or halted using appropriate engineering technologies to stop excessive pumping and reduce the fluctuation of the piezometric level.

The perspectives of our work could consist of the following:

- The adoption of a combined model with GPR, ERT, and radar interferometry techniques and the mobilization of additional variables and tools.
- The expansion of the spatial extent of the survey to the entire Setifian high plain region.
- The identification of the characteristics of all listed sinkholes and if there is any correlation between their shapes.
- The integration of the MPQ-geomorphic dynamics to identify more clearly the distribution of sinkholes.

Acknowledgements

The International Association of Water Resources in the Southern Mediterranean Basin-Tunisia oversaw this work. The authors appreciate the support of the Water and Environment laboratory at Tebessa University. Acknowledgments, to the General Directorate of Scientific Research and Technological Development (DGRSDT-MESRS) for the technical support. Tribute to the editor and reviewers for their valuable improvement on the manuscript.

Conflicts of interest statement

On behalf of all authors, the corresponding author states that there are no conflicts of interest. All participating authors have not a financial or personal relationship with a third party whose interests could be positively or negatively influenced by the article's content.

References

Anis Z., Wissem G., Riheb H., Biswajeet P., Essghaier G.M. 2019. Effects of clay properties in the landslide's genesis in flysch massif: Case study of Aïn Draham, Northwestern Tunisia. Journal of African Earth Sciences, 151, 146–152.

Benmarce K., Hadji R., Zahri F., Khanchoul K., Chouabi A., Zighmi K., Hamed Y. 2021. Hydrochemical and geothermometry characterization for a geothermal system in semiarid dry climate: The case study of Hamma spring (northeast Algeria). Journal of African Earth Sciences, 104285.

Besser H., Mokadem N., Redhaounia B., Hadji R., Hamad A., Hamed Y. 2018. Groundwater mixing and geochemical assessment of low-enthalpy resources in the geothermal field of southwestern Tunisia. Euro-Mediterranean Journal for Environmental Integration, 3(1), 16.

Besser H., Dhaouadi L., Hadji R., Hamed Y., Jemmali H. 2021. Ecologic and economic perspectives for sustainable irrigated agriculture under arid climate conditions: An analysis based on environmental indicators for southern Tunisia. Journal of African Earth Sciences, 177, 104134.

Brahmi S., Baali F., Hadji R., Brahmi S., Hamad A., Rahal O., ... Hamed Y. 2021. Assessment of groundwater and soil pollution by leachate using electrical resistivity and induced polarization imaging survey, case of Tebessa municipal landfill, NE Algeria. Arabian Journal of Geosciences, 14(4), 1–13.

Chemseddine F., Dalila B., Fethi B. 2015. Characterization of the main karst aquifers of the Tezbent Plateau, Tebessa Region, Northeast of Algeria, based on hydrogeochemical and isotopic data. Environmental Earth Sciences, 74(1), 241–250.

Dahlin T., Zhou B. 2004. A numerical comparison of 2D resistivity imaging with ten electrode arrays. Geophysical Prospecting, 52(5), 379–398.

Dahoua L., Savenko V.Y., Hadji R. 2017. GIS-based technic for roadside-slope stability assessment: A bivariate approach for A1 East-west highway. North Algeria. Mining Science, 24, 81–91.

Dahoua L., Yakovitch S.V., Hadji R., Farid Z. 2017b. Landslide Susceptibility Mapping Using Analytic Hierarchy Process Method in BBA-Bouira Region. Case Study of East-West Highway, NE Algeria.

Demdoum A., Hamed Y., Feki M., Hadji R., Djebbar M. 2015. Multi-tracer investigation of groundwater in El Eulma Basin (Northwestern Algeria), North Africa. Arabian Journal of Geosciences, 8(5), 3321–3333.

El Mekki A., Hadji R., Chemseddine F. 2017. Use of slope failures inventory and climatic data for landslide susceptibility, vulnerability, and risk mapping in souk Ahras region. Mining Science, 24.

Fehdi C., Baali F., Boubaya D., Rouabhia A. 2011. Detection of sinkholes using 2D electrical resistivity imaging in the Cheria Basin (north–east of Algeria). Arabian Journal of Geosciences, 4(1–2), 181–187.

Ford D., Williams P.D. 2013. Karst hydrogeology and geomorphology. John Wiley & Sons.

Fredj M., Hafsaoui A., Riheb H., Boukarm R., Saadoun A. 2020. Back-analysis study on slope instability in an open pit mine (Algeria). Natsional'nyi Hirnychyi Universytet. Naukovyi Visnyk, (2), 24–29.

Gaballah M., Alharbi T. 2022. 3-D GPR visualization technique integrated with electric resistivity tomography for characterizing near-surface fractures and cavities in limestone. Journal of Taibah University for Science, 16(1), 224–239.

Giampaolo V., Capozzoli L., Grimaldi S., Rizzo E. 2016. Sinkhole risk assessment by ERT: The case study of Sirino Lake (Basilicata, Italy). Geomorphology, 253, 1–9.

Hadji R., Boumazbeur A., Limani Y., Baghem M., Chouabi A. 2013. Geologic, topographic, and climatic controls in landslide hazard assessment using GIS modeling: A case study of Souk Ahras region, NE Algeria. Quaternary International, 302, 224–237.

Hadji R., Limani Y., Boumazbeur A., Demdoum A., Zighmi K., Zahri F., Chouabi A. 2014a. Climate change and their influence on shrinkage – swelling clays susceptibility in a semi – arid zone: A case study of Souk Ahras municipality, NE-Algeria. Desalination and Water Treatment, 52 (10–12), 2057–2072.

Hadji R., Limani Y., Demdoum A. 2014b. Using multivariate approach and GIS applications to predict slope instability hazard case study of Machrouha municipality, NE Algeria. 10.1109/ICT-DM.2014.6917787. IEEE Xplore. 14651190.

Hadji R., Chouabi A., Gadri L., Raïs K., Hamed Y., Boumazbeur A. 2016. Application of linear indexing model and GIS techniques for the slope movement susceptibility modeling in Bousselam upstream basin, Northeast Algeria. Arabian Journal of Geosciences, 9, 192.

Hadji R., Raïs K., Gadri L., Chouabi A., Hamed Y. 2017. Slope failures characteristics and slope movement susceptibility assessment using GIS in a medium scale: A case study from Ouled Driss and Machroha municipalities, Northeastern of Algeria. Arabian Journal for Science and Engineering, 42, 281–300.

Hamad A., Baali F., Hadji R., Zerrouki H., Besser H., Mokadem N., ... Hamed Y. 2018a. Hydrogeochemical characterization of water mineralization in Tebessa-Kasserine karst system (Tuniso-Algerian Transboundary basin). Euro-Mediterranean Journal for Environmental Integration, 3(1), 7.

Hamad A., Hadji R., Bâali F., Houda B., Redhaounia B., Zighmi K., ... Hamed Y. 2018b. Conceptual model for karstic aquifers by combined analysis of GIS, chemical, thermal, and isotopic tools in Tuniso-Algerian transboundary basin. Arabian Journal of Geosciences, 11(15), 409.

Hamad A., Hadji R., Boubaya D., Brahmi S., Baali F., Legrioui R., ... Hamed Y. 2021. Integrating gravity data for structural investigation of the Youkous-Tebessa and Foussana-Talah transboundary basins (North Africa). Euro-Mediterranean Journal for Environmental Integration, 6(2), 1–11.

Hamed Y., Redhaounia B., Ben Sâad A., Hadji R., Zahri F. 2017b. Groundwater inrush caused by the fault reactivation and the climate impact in the mining Gafsa basin (SW Tunisia). Journal of Tethys, 5(2), 154–164.

Hamed Y., Redhaounia B., Sâad A., Hadji R., Zahri F., Zighmi K. 2017a. Hydrothermal waters from karst aquifer: Case study of the Trozza basin (Central Tunisia). Journal of Tethys, 5(1), 33–44.

Hamed Y., Hadji R., Redhaounia B., Zighmi K., Bâali F., El Gayar A. 2018. Climate impact on surface and groundwater in North Africa: A global synthesis of findings and recommendations. Euro-Mediterranean Journal for Environmental Integration, 3(1), 25.

Hamed Y., Hadji R., Ncibi K., Hamad A., Ben Saad A., Melki A., ... Mustafa E. 2022. Modelling of potential groundwater artificial recharge in the transboundary Algero-Tunisian Basin (Tebessa-Gafsa): The application of stable isotopes and hydro informatics tools. Irrigation and Drainage, 71(1), 137–156.

Karim Z., Hadji R., Hamed Y. 2019. GIS-based approaches for the landslide susceptibility prediction in Setif Region (NE Algeria). Geotechnical and Geological Engineering, 37(1), 359–374.

Khaldaoui F., Djeddi M., Djediat Y., Ydri A. 2015. Geophysical study of the mechanism of sinkhole formation in north-east Algeria. International Conference on Engineering Geophysics, Al Ain, United Arab Emirates, 15–18 November 2015, 126–128. Society of Exploration Geophysicists.

Kidanu S.T., Torgashov E.V., Varnavina A.V., Anderson N.L. 2016. ERT-based investigation of a sinkhole in Greene County, Missouri. AIMS Geosci, 2(2), 99–115.

Loke M.H., Wilkinson P.B., Chambers J.E., Strutt M. 2014. Optimized arrays for 2D cross-borehole electrical tomography surveys. Geophysical Prospecting, 62(1), 172–189.

Mahdadi F., Boumezbeur A., Hadji R., Kanungo D.P., Zahri F. 2018. GIS-based landslide susceptibility assessment using statistical models: A case study from Souk Ahras province, NE Algeria. Arabian Journal of Geosciences, 11(17), 476.

Manchar N., Benabbas C., Hadji R., Bouaicha F., Grecu F. 2018. Landslide Susceptibility Assessment in Constantine Region (NE Algeria) by Means of Statistical Models. Studia Geotechnica et Mechanica, 40(3), 208–219.

Mokadem N., Demdoum A., Hamed Y., Bouri S., Hadji R., Boyce A., Laouar R., Saad A. 2016. Hydrogeochemical and stable isotope data of groundwater of a multi-aquifer system: Northern Gafsa basin e Central Tunisia, Journal of African Earth Sciences, 114, 174–191.

Mouici R., Baali F., Hadji R., Boubaya D., Audra P., Fehdi C.É., ... Arfib B. 2017. Geophysical, geotechnical, and speleologic assessment for karst-sinkhole collapse genesis in Cheria plateau (NE Algeria). Mining Science, 24, 59–71.

Ncibi K., Chaar H., Hadji R., Baccari N., Sebei A., Khelifi F., ... Hamed Y. 2020a. A GIS-based statistical model for assessing groundwater susceptibility index in shallow aquifer in Central Tunisia (Sidi Bouzid basin). Arabian Journal of Geosciences, 13(2), 98.

Ncibi K., Hadji R., Hajji S., Besser H., Hajlaoui H., Hamad A., ... Hamed Y. 2021. Spatial variation of groundwater vulnerability to nitrate pollution under excessive fertilization using index overlay method in central Tunisia (Sidi Bouzid basin). Irrigation and Drainage.

Ncibi K., Hadji R., Hamdi M., Mokadem N., Abbes M., Khelifi F., ... Hamed Y. 2020b. Application of the analytic hierarchy process to weight the criteria used to determine the Water Quality Index of groundwater in the northeastern basin of the Sidi Bouzid region, Central Tunisia. Euro-Mediterranean Journal for Environmental Integration, 5, 1–15.

Nouioua I., Rouabhia A., Fehdi C., Boukelloul M.L., Gadri L., Chabou D., Mouici R. 2013. The application of GPR and electrical resistivity tomography as useful tools in detection of sinkholes in the Cheria Basin (northeast of Algeria). Environmental Earth Sciences, 68(6), 1661–1672.

Olayinka A.I., Yaramanci U. 2000. Assessment of the reliability of 2D inversion of apparent resistivity data. Geophysical Prospecting, 48(2), 293–316.

Raïs K., Kara M., Gadri L., Hadji R., Khochman L. 2017. Original approach for the drilling process optimization in open cast mines: Case study of Kef Essenoun open pit mine Northeast of Algeria. Mining Science, 24, 147–159.

Saddek B., Chemseddine F., Djamel B., Nabil B. 2019. Surface and Subsurface Investigations for the Detection and Mapping of Underground Karst. Journal of the Geological Society of India, 93(2), 228–234.

Talib O.C., Shimon W., Sarah K., Tonian R. 2022. Detection of sinkhole activity in West-Central Florida using InSAR time series observations. Remote Sensing of Environment, 269, 112793.

Tamani F., Hadji R., Hamad A., Hamed Y. 2019. Integrating remotely sensed and GIS data for the detailed geological mapping in semi-arid regions: Case of Youks les Bains Area, Tebessa Province, NE Algeria. Geotechnical and Geological Engineering, 37(4), 2903–2913.

Van Schoor M. 2002. Detection of sinkholes using 2D electrical resistivity imaging. Journal of Applied Geophysics, 50(4), 393–399.

Watlet A., Kaufmann O., Triantafyllou A., Poulain A., Chambers J.E., Meldrum P.I., Van Camp M. 2018. Imaging groundwater infiltration dynamics in the karst vadose zone with long-term ERT monitoring. Hydrology and Earth System Sciences, 22(2), 1563–1592.

Zahri F., Boukelloul M., Hadji R., Talhi K. 2016. Slope stability analysis in open pit mines of jebel Gustar Career, Ne Algeria. A Multi-Steps Approach. Mining Science, 23, 137–146.

Zeqiri R.R., Riheb H., Karim Z., Younes G., Mania B., Aniss M. 2019. Analysis of safety factor of security plates in the mine "Trepça" Stantërg. Mining Science, 26, 21.

Prof. Riheb Hadji (Corresponding Author)
Earth Sciences Department,
Laboratory of Applied Research in Engineering Geology, Geotechnics, Water Sciences, and Environment
Ferhat Abbas University, Setif 19137, Algeria
e-mail: hadjirihab@yahoo.fr
ORCID: 0000-0002-9632-0812

PhD Serhane Brahmi
Department of Earth Sciences, Water and Environment Laboratory
Larbi Tebessi University, Tebessa, Algeria
e-mail: serhanebrahmi@univ-tebessa.dz

Prof. Fehdi Chemseddine
Department of Earth Sciences, Water and Environment Laboratory
Larbi Tebessi University, Tebessa, Algeria
e-mail: fehdi.chemseddine@univ-tebessa.dz

PhD Smail Brahmi
Department of Earth Sciences, Water and Environment Laboratory
Larbi Tebessi University, Tebessa, Algeria
e-mail: smail.brahmi@univ-tebessa.dz

PhD Amor Hamad
Department of Earth Sciences, Water and Environment Laboratory
Larbi Tebessi University, Tebessa, Algeria
e-mail: hsamir2001@gmail.com

Prof. Younes Hamed
Earth Sciences, Faculty of Sciences, University of Gafsa, Tunisia
International Association of Water Resources in the Southern Mediterranean Basin
e-mail: hamed_younes@yahoo.fr